Proposal for a Forward Neutron Calorimeter for the H1 Experiment at DESY

H1-Collaboration *

M. Beck, W. Brückner, Th. Haller, D.M. Jansen, F. Metlica,
T. Nunnemann, B. Povh, R. Todenhagen

Max-Planck Institut für Kernphysik, Postfach 103980,
69029 Heidelberg, Germany

(August 7, 1995)

Abstract

At HERA, the reaction $ep \to e'nX$ can be studied. In a properly chosen kinematic domain, it is expected that this reaction will be dominated by deep inelastic scattering (DIS) on a pion coupled to the ground state or excited states of the proton. A forward neutron calorimeter in conjunction with the H1 experiment at HERA, can be used to study these interactions and to measure the pion structure function. In addition, the fraction of large rapidity-gap events ascribed to pion exchange can be measured. A proposal for installation of a forward neutron calorimeter for the H1 Experiment at DESY is described in this paper.

Introduction

We propose to add a new forward neutron calorimeter to the H1 experiment at DESY. The purpose of the new neutron calorimeter is to measure the energy and angle of produced neutrons with high precision. The calorimeter will be situated 107 m from the interaction point at zero degrees with respect to the incident proton direction. Measurement of the forward neutron angle and energy, along with the determination of the scattered electron and the hadronic jets, will to a large extent specify the kinematics of the reaction $ep \to e'nX$. This paper describes the physics motivation and design specifications for the neutron calorimeter.

Physics Motivation

Many theoretical papers have discussed the possibility of measuring the pion structure function at HERA [1–5]. The pion cloud around the nucleon can contribute to the deep

*Subject to approval by the collaboration board on September 6, 1995 inelastic scattering structure functions of the proton via the $ep \to e'nX$ process shown in Figure 1. Four Lorentz invariants are needed to completely specify the reaction. One convenient set is

$$t = (p-p')^2, \quad z = 1 - \frac{2k\cdot(p-p')}{s}, \quad Q^2 = -(k-k')^2, \quad \text{and} \quad y = \frac{2p\cdot(k-k')}{s}. \tag{1}$$

These Lorentz invariants are symmetric with respect to the lepton and baryon currents. The four-momentum transfer t, written in terms of p_T the transverse momentum of the final-state neutron, is equal to

$$t = -\frac{p_T^2}{z} - (1-z)(\frac{m_n^2}{z} - m_p^2) \tag{2}$$

With the proposed neutron calorimeter, which will measure the neutron's energy and production angle, a precise determination of the t distribution for the reaction shown in Figure 1 is possible.

The pion-exchange model is used to calculate the DIS cross section on the pion. The model has been tested using the reaction $\pi p \to nX$. The differential cross section for this reaction factorizes and takes the form

$$\frac{d\sigma(\pi p \to nX)}{dz\, dp_T^2} = \frac{2}{3}\, f_{n/p}(z, p_T^2)\, \sigma_{\pi\pi}(s_{\pi\pi}) \tag{3}$$

where $\sigma_{\pi\pi}(s_{\pi\pi})$ is the $\pi\pi$ total cross section and $f_{n/p}(z, p_T^2)$ is the flux of neutrons with transverse momentum p_T and the fraction z of the proton's momentum [1]. Experimental data are well described by this equation [3]. An important point is that the flux of neutrons $f_{n/p}(z, p_T^2)$ is a universal property of the proton which does not depend upon the incident projectile. The flux factor is equal to

$$f_{n/p}(z, p_T^2) = \frac{3g^2_{p\pi^0 p}}{16\pi^2} \frac{[(1-z)^2 m_n^2 + p_T^2]}{z^2(1-z)(m_N^2 - M_{\pi p}^2)^2} |F(z, p_T^2)|^2 \tag{4}$$

where $F(z, p_T^2)$ is the vertex form factor and $g^2_{p\pi^0 p})/4\pi = 13.6$ is the strong coupling constant determined from low-energy physics. In Figure 2 we show the flux factor as a function of z integrated over $0 < p_T^2 < 2$ $(\mathrm{GeV/c})^2$.

At HERA, it is expected that pion exchange will play a dominant role in the reaction $ep \to e'nX$. Using the same formalism as above, the cross section is given by

$$\frac{d\sigma(ep \to e'nX)}{dx\, dQ^2\, dz\, dp_T^2} = \frac{2}{3}\, f_{n/p}(z, p_T^2)\, K(x, Q^2)\, F_2^{e\pi}(x_\pi, Q^2) \tag{5}$$

where $F_2^{e\pi}(x_\pi, Q^2)$ is the structure function of the pion and $K(x, Q^2)$ is the kinematical factor

$$K(x, Q^2) = \frac{4\pi\alpha^2}{Q^4}\frac{1}{x}[1 - y + \frac{1}{2}y^2]. \tag{6}$$

The Bjorken variable in the electron-pion deep inelastic scattering is $x_\pi = x/(1-z)$ and $y = Q^2/(xs)$.

In Figure 3 we show four different parametrizations of the pion structure function as a function of x_π. The curves were calculated using PDFLIB [6]. There is a large variation in the predictions for $x_\pi < 0.1$. At the present time, the pion structure function has only been well determined at large x_π using Drell-Yan experimental data [7]. At HERA, if the virtual pion can be effectively "tagged", the pion structure function can be measured directly down to $x_\pi \approx 10^{-4}$. In Figure 4 we show the cross section $d\sigma(ep \to e'nX)/(dx\, dQ^2\, dz\, dp_T^2)$ as a function of p_T^2 and z for $x = 0.001$ and $Q^2 = 10$ GeV^2. The SMRS-P2 pion parton distributions were used in the calculation.

Rate estimates for pion exchange have been calculated. The Monte Carlo integration program Vegas [8] has been used to integrate Equation 5. In Table I, we show the pion exchange cross section integrated over $0 < z < 1$, $10 < Q^2 < 100$ GeV^2, $0.0001 < x < 1$, and $0 < p_T^2 < 2$ (GeV/c)^2. The DIS cross section, calculated using Lepto 6.1 [9], is also shown. The DIS cross section is integrated over $0.0001 < x < 1$ and $10 < Q^2 < 100$ GeV^2. Comparing the cross sections, one expects that approximately 20% of all DIS events will have a final-state neutron. This number of events is suitable to determine the fraction of large rapidity events caused by pion exchange.

Estimation of the rate due to meson exchange with higher masses (for example ρ and a_2) can also be calculated. In Figure 6, the pion-exchange contribution to $dF_2^{p\to n}(x, Q^2)/dzdp_T^2$ and the background, provided by ρ and a_2 exchanges, is shown as functions of z. The ratio is shown for different values of the transverse momentum p_T^2. At $p_T^2 = 0$ (GeV/c)^2 and $z = 0.8$, pion exchange is approximately 20 times larger than the contribution due to ρ and a_2 exchange [10].

To estimate the number of events that could be used to evaluate the pion structure function, we restrict ourselves to the limited kinematic range $0.7 < z < 0.9$, $10 < Q^2 < 20$ GeV^2, $0.0001 < x < 1$, and $0 < p_T^2 < 0.16$ (GeV/c)^2. In this kinematic range, we expect that the foward neutron calorimeter will have about 50% acceptance and that the background contributions due to ρ and a_2 exchange will be small. Assuming 10 pb^{-1} luminosity, one expects approximately 6000 reconstructed events. In Figure 7, we show how these events are distributed as a function of x. In Figure 3 the expected statistical accuracy which can be obtained with the forward neutron calorimeter, for data with $10 < Q^2 < 15$ GeV^2, is shown.

Because of the short amount of available time, the calorimeter will be calibrated with a low energy (15 GeV) e, π, and p test beam at CERN. The upper part of the calorimeter will be put in the X1 test beam at CERN next year in order to have 120 GeV e calibration. Prior to this time, we can not correctly estimate the systematic errors associated with the energy calibration.

Neutron Calorimeter Specifications

Neutrons stemming from the process described above, will have momenta between about 200 GeV/c and the maximum of 820 GeV/c. Their angles with respect to the incoming proton direction will be less than 1 mrad. 100 m away from the interaction point this translates into a circular distribution of neutron impacts with radius of 10 cm around the 0° line at the calorimeter front face.

To measure those neutrons with adequate precision, we want to use a hadronic calorimeter based on the Pb/scintillating fiber technique. The calorimeter we envisage is the SPACAL, which was developed in the framework of the CERN/LAA project [11] and subsequently has been used in the CERN hyperon beam experiment WA89 [12]. This calorimeter consists of a Pb structure with interleaved layers of 2.2 m long scintillating fibers in a geometry as shown in figure 8. The fiber diameter is 1 mm and their spacing is 2.22 mm giving a Pb to fiber ratio of 4:1. Particles enter the front face (almost) parallel to the fibers and develop a shower inside the 9.5 interaction lengths deep detector ($\lambda_I \approx 21$ cm). The calorimeter is laterally segmented in 155 hexagonal towers (Figure 9). Each tower is defined by 1141 fibers which are coupled to a common photomultiplier (PM) located on the rear of the calorimeter. The diameter of the active area is about 95 cm corresponding to 4.5 λ_I.

In order to reject showers that are initiated by charged particles, as well as events where a neutron preshowered in some other part of the detector, a scintillating tile hodoscope (SCITIL) is placed about 15 cm in front of the SPACAL. This hodoscope is made out of 127 hexagonal tiles (Figure 10) and has a granularity identical to the one given by the tower structure of the calorimeter. The individual scintillator tiles are read out via wave length shifting fibers that are coupled to PMs located outside the active area of the SCITIL/SPACAL detectors. The efficiency of the hodoscope to the passage of charged particles was determined to be $\geq 98\%$. It's properties are described in more details in [13].

The properties of SPACAL have been measured extensively. Some of those, which are of importance for the application described in this paper are reviewed in the following section.

Testbeam results

The results presented in this section are based on the analysis of data, taken in a e^-/π^- testbeam with an energy range of 5-150 GeV. Details can be found in [11,14–18]

- Energy resolution

  Due to the light attenuation in the fibers, neutrons showering close to the PMs will produce a higher signal, than those showering close to the front face. Thus the energy distribution measured with the calorimeter is broadened. Correcting for this effect, one obtains an energy resolution of the following form:

  $\frac{\sigma}{E} = \frac{(30.6 \pm 0.5)\%}{\sqrt{E[GeV]}} + (1.0 \pm 0.1)\%$. [16]

  Neglecting the light attenuation gives a slightly higher constant term of $(2.5 \pm 0.1)\%$, whereas the scaling term is reduced to $(27 \pm 0.6)\%$.

- Position resolution

  The resolution of the impact point measurement for hadrons was determined with pions entering the central region of a SPACAL tower at an angle of 3° with respect to the normal on the calorimeter front face. The data can be parameterized as $\sigma_y(E) = 2.4 + 31.4/\sqrt{E[GeV]}\ [mm]$ [15]. The angular dispersion of the proton beam at the neutron calorimeter is $\sigma_v = 9$ mm and $\sigma_h = 3$ mm. Such a resolution allows us to measure the neutron angle with a precision of 100 μrad at an energy of 500 GeV.

- Linearity

  Several effects may contribute to a possible alinearity of the SPACAL. a) Light attenuation in the fibers. As the average shower depth of a hadronic shower is increasing with energy, light produced in a high energy shower will be less affected by attenuation in the fibers, than light from low energy showers. b) Energy leakage out of the detector. Like the average shower depth the length of 95 % longitudinal containment of the shower is increasing with energy. Thus for high energy showers a larger fraction of shower energy will remain undetected from the calorimeter. In addition to these more general effects the specific testbeam setup as described in [16] reveals two other contributions to the alinearity: c) Energy loss in the pre shower detector. d) Low energy cutoff. After correction of the effects a) - d) the signal per GeV increased by $\sim$ 5 % over the energy range 5-150 GeV.

- Compensation

  The ratio of scintillation light per GeV deposited energy produced by the electromagnetic (e.m.) and non-e.m. components of a hadronic shower is called e/h. The large and non-Gaussian fluctuations in the fraction of e.m. energy generated in hadronic showers only vanishes in case of compensation (e/h = 1). Therefore the SPACAL was designed to be compensating. For the particular choice of fibers and sampling fraction, the e/h was found to be 1.15 ± 0.02 [16].

- Signal speed and influence of the ADC gate width

  Due to the negligible cross section for thermal neutron capture, characteristic for Uranium calorimeters), the signal speed of the SPACAL is extremely fast. More than 90 % of the charge of a 80 GeV hadronic shower is collected within 50 ns. Nevertheless long cables affect these numbers. In the WA89 experiment a cable-length of 120 m was used. In order to avoid negative influences on energy and position resolution an effective ADC gate of 100 ns was chosen (ADC LeCroy 1882F 12bit with 3bit range switching). As the foreseen use within the H1 experiment features low rates in the order of a few events per second, pile up effects can safely be neglected. The use of 100 MHz flash ADCs (Struck F1002) of 8 bit resolution (sampling the signal approximately 16 times) should be appropriate to achieve results that are comparable with those of the testbeam.

Modifications to the Calorimeter SPACAL

The current layout of the calorimeter is shown in Figure 9. The limitation of installation space in the HERA accelerator tunnel requires the overall width to be less than 80cm. The maximum weight of anything being transported into the HERA tunnel must not exceed 10 t. Thus, the Pb matrix of the current calorimeter (weight 19 t) has to be reduced in size. Furthermore the proton beampipe is located just 18 cm above the 0° neutron impact, generating the need for a beam hole within the calorimeter.

In order to achieve a simple installation as well as a simple modification we developed a possible configuration, shown in Figure 11. In this setup the calorimeter is split into a lower and an upper part. Once the upper part is placed on top of the lower one, there is a 'one-module' gap, providing enough space for the proton beamline to pass through. The weight of the lower part's Pb matrix is 7.5 t, leaving enough safety to stay below 10 t once support, PMs and SCITIL are mounted. As the Pb/fiber matrix is built by stacking engrooved sheets of Pb (49.5 mm $\times$ 1.92 mm $\times$ 2000 mm) on top of each other (as shown in Figure 8) the majority of modules stays untouched and only a small fraction of the existing modules have to be rebuilt. The upper part is designed to be small and light (less than 2 t), as easy proton beam pipe access may be a condition by the HERA accelerator group. A possible scenario is a lifting mechanism attached to the ceiling of the HERA tunnel.

Modifications to the hodoscope SCITIL

Due to the modular structure of the scintillating tile hodoscope SCITIL (Figure 10), building the hodoscope for the FNC is just a matter of rearranging the SCITIL modules. A possible setup is shown in Figure 12. As the FNC needs to be split in two parts, all PM tubes of the lower part have to be mounted underneath the sensitive area. Four PM mounting layers have to be stacked in depth to fit all PMs into the mounting volume.

Data Acquisition and Slow Control

The calorimeter and hodoscope modules will be digitized in F1002 Flash ADCs, similar to the Flash ADC systems that are already installed in H1. We expect 1800 data bytes per event after data reduction by a DESY standard F1004 Scanner. There will be a dedicated special VME crate (F1000) to house flash ADCs and scanner. The readout will be done via a standard VME/VSB connection to the main H1 data acquisition. A second VME/VSB interface will connect to the Spacal slow control, an Alpha workstation. The Spacal slow control will connect to the main H1 slow control via Ethernet.

Logistics

A proposed time schedule for work that will be done on the neutron calorimter is given in Table II.

- The mechanical support in the HERA tunnel for the neutron calorimeter will be built by DESY.
- Mechanical engineering and construction will be done by Max-Planck Institut für Kernphysik, Heidelberg.
- The new version of the calorimeter will be built at CERN where space has been provided.
- The modules will be tested and adjusted using a 15 GeV e, π, and p test beam at CERN.
- In the beginning of 1996, the calorimeter will be brought to DESY.
- Electronics up to the interface with the H1 experiment is taken care of by the Max-Planck Institut für Kernphysik, Heidelberg.

Cost Estimate

Much of the detector hardware needed for the neutron calorimeter is already existing. The high voltage crates, cards, adapter panels, and interface, used in the CERN experiment WA89, will be re-used again. A cost estimate for new materials that must be purchased for the project amounts to about D.M. 323.000, details are given in Table III. Technical support, consisting of three technicians working for two months, is also necessary with a cost of D.M. 27.000.

Summary

From the above considerations, we conclude that it will be possible to start taking data with the calorimeter at the beginning of the 1996 run period.

REFERENCES

[1] H. Holtmann *et al.*, Phys. Lett. **B338**, 363 (1994).
[2] H. Holtmann *et al.*, Jülich preprint KFA-IKP(TH)-1993-33, submitted to Phys. Rev. D.
[3] G. Levman and K. Furutani,"Virtual Pion Scattering at HERA", ZEUS-Note 92-107.
[4] R. Zoller, Z. Phys. **C53**, 443 (1992).
[5] J. D. Sullivan, Phys. Rev. D **5**, 1732 (1972).
[6] H. Plothow-Besch/CERN-PPE, W5051 PDFLIB, 1994.03.11.
[7] D. McCal *et al.*, Phys. Lett. **85B**, 432 (1979);
C. B. Newman *et al.*, Phys. Rev. Lett. **42**, 951 (1979).
[8] G. P. Lepage, J. Comp. Phys. 27,192 (1978).
[9] T. Sjostrand, "The Lund Monte Carlo for Jet Fragmentation and e+e- Physics: Program Manual", July 1990.
[10] B. Kopeliovich, private communication.
[11] D. Acosta *et al.*, Nucl. Instr. and Meth. A294 (1990) 193.
[12] M. Beck *et al.*, MPI preprint MPIH-V16-1995, submitted to Nucl. Instr. and Meth. A.
[13] M. Beck *et al.*, Nucl. Instr. and Meth. A355 (1995) 351.
[14] D. Acosta *et al.*, Nucl. Instr. and Meth. A302 (1991) 36.
[15] D. Acosta *et al.*, Nucl. Instr. and Meth. A305 (1991) 55.
[16] D. Acosta *et al.*, Nucl. Instr. and Meth. A308 (1991) 481.
[17] D. Acosta *et al.*, Nucl. Instr. and Meth. A314 (1992) 86. Search for: 308
[18] D. Acosta *et al.*, Nucl. Instr. and Meth. A316 (1992) 184.

TABLES

Pion exchange σ	PDF	Deep inelastic scattering σ	PDF
22 nb	GRV-P LO	75 nb	Morfin-Tung Set 1
12 nb	OW-P Set 1	77 nb	Duke-Owens Set 1
13 nb	SMRS-P 2	130 nb	Glück-Reya-Vogt LO Set
19 nb	ABFKW-P Set 1	66 nb	EHLQ Set 1

TABLE I. Comparison of pion exchange and DIS cross section. See text for details.

Work	Time estimate	Institution
Modify lead/fibre matrix	15/08/95 – 15/10/95	M.P.I.
15 GeV π,e,p testbeam	01/11/95 – 15/11/95	M.P.I/CERN
Ship calorimeter to DESY	01/1/96 – 15/1/96	M.P.I.
Install calorimeter in beamline	16/1/96 – 30/1/96	M.P.I./DESY
Integrate with H1 DAQ system	01/2/96 – 30/2/96	M.P.I/DESY

TABLE II. Proposed time schedule for work that will done on the forward neutron calorimeter.

Item	Description	Cost per Item (D.M.)	Total Cost (D.M.)
11 Flash ADC's F1002	with accessories	—	169.037
90 Photomultipliers	XP 2282 B	560	50.400
Alpha Workstation	with accessories	33.750	33.750
2 Hard Disks	9 gigabytes	4020	8.040
192 Signal cables	150 m long	130	25.100
8 High Voltage cables	150 m long	3125	25.000
32 High Voltage connectors	lemo connectors	300	9.600
384 Signal connectors	bnc connectors	4	1.600

TABLE III. Cost estimate for new materials that must be purchased for the neutron calorimeter. The total cost is 322.527 D.M. The accessories for the Flash ADC's consist of a crate (F1000), a scanner (F1004), power supplies, and spares.

FIGURES

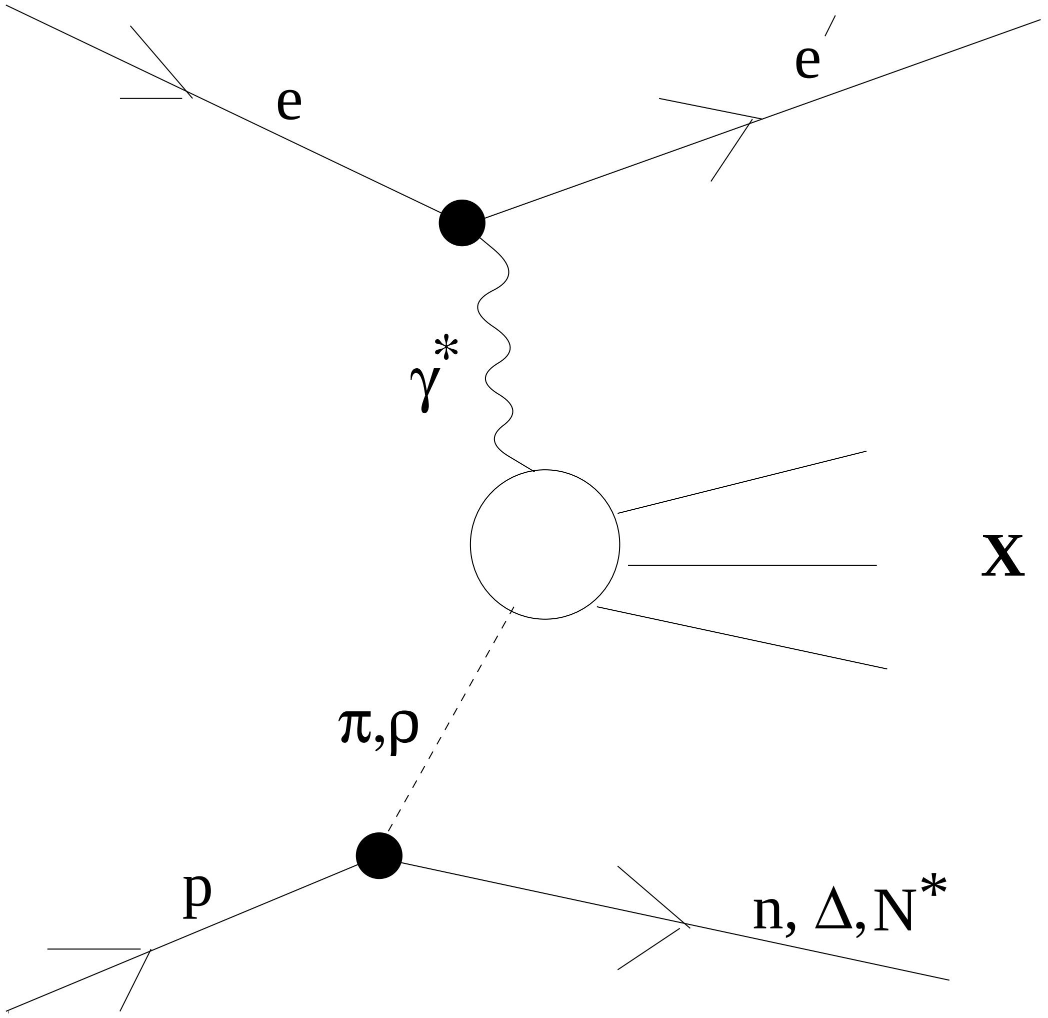

FIG. 1. The pion exchange contribution to deep inelastic scattering.

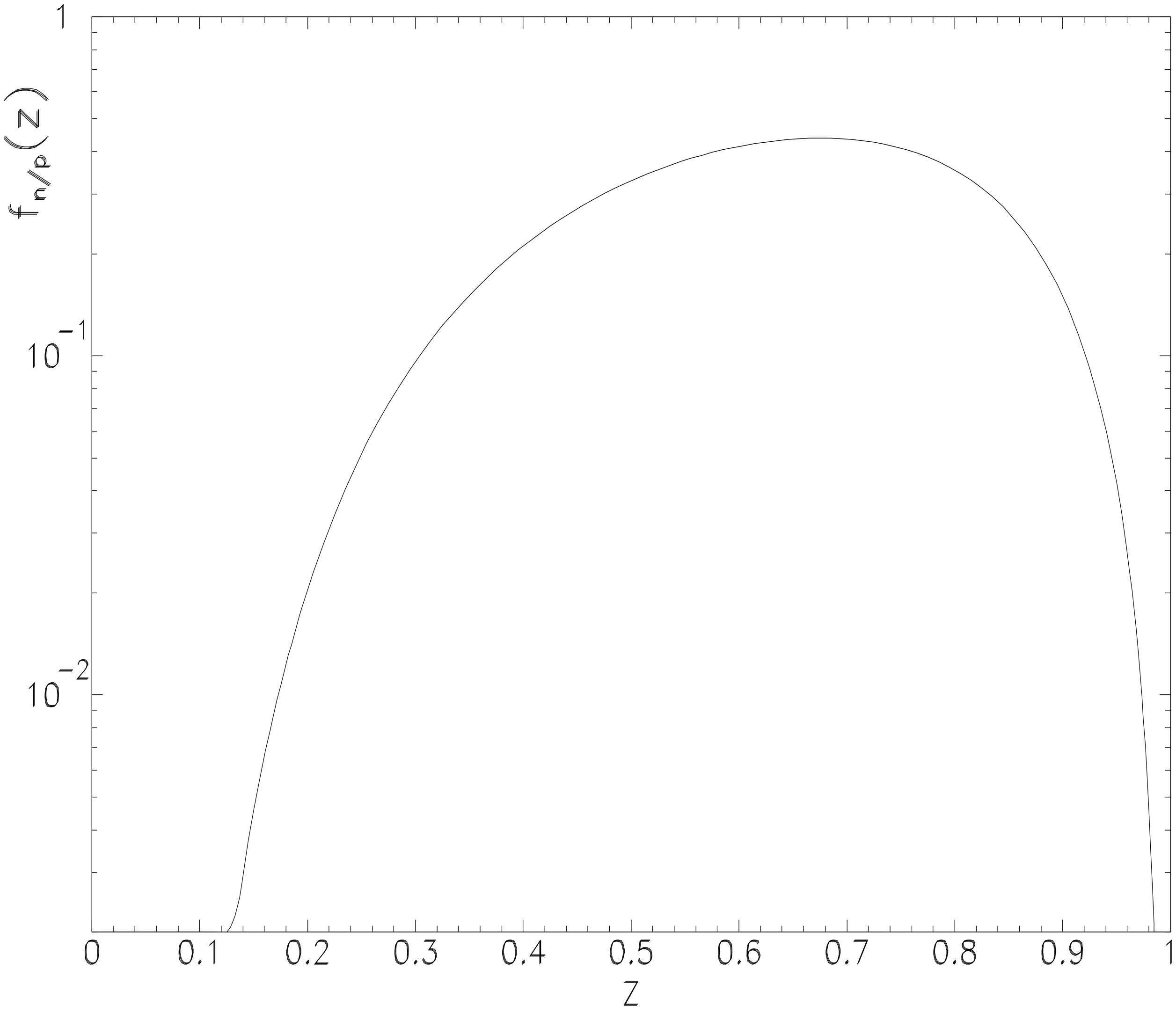

FIG. 2. The flux of neutrons $f_{n/p}(z, p_T^2)$ as a function of z. The transverse momentum has been integrated over $0 < p_T^2 < 2$ (GeV/c)^2.

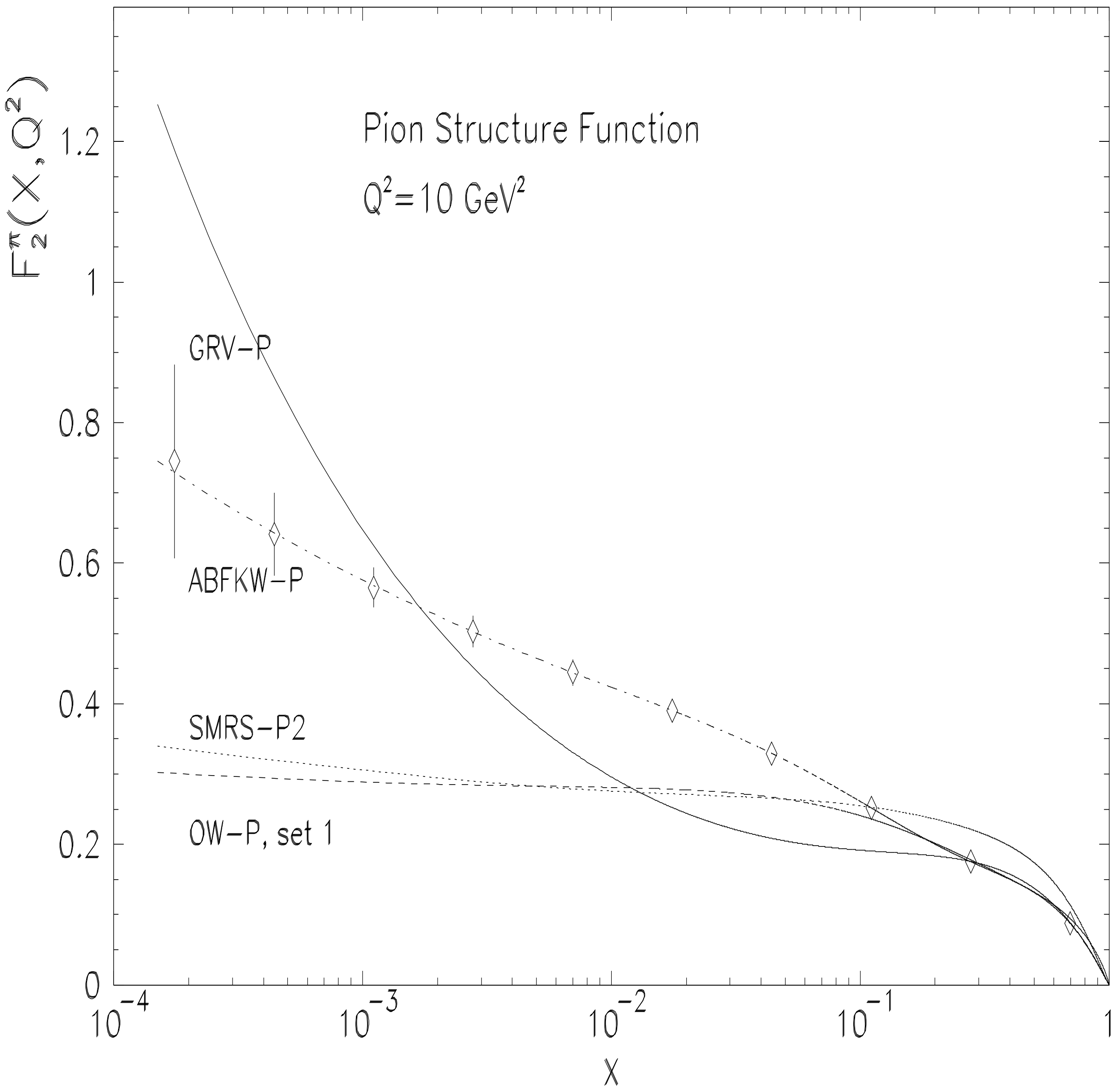

FIG. 3. The pion structure function $F_2(x,Q^2)$ as a function of x. The expected statistical accuracy which can be obtained with the forward neutron calorimeter, assuming a luminosity of 10 pb^{-1} and 50% acceptance, is shown by the data points. The Q^2 range for the data is $10 < Q^2 < 15$ GeV^2. See also Figure 7.

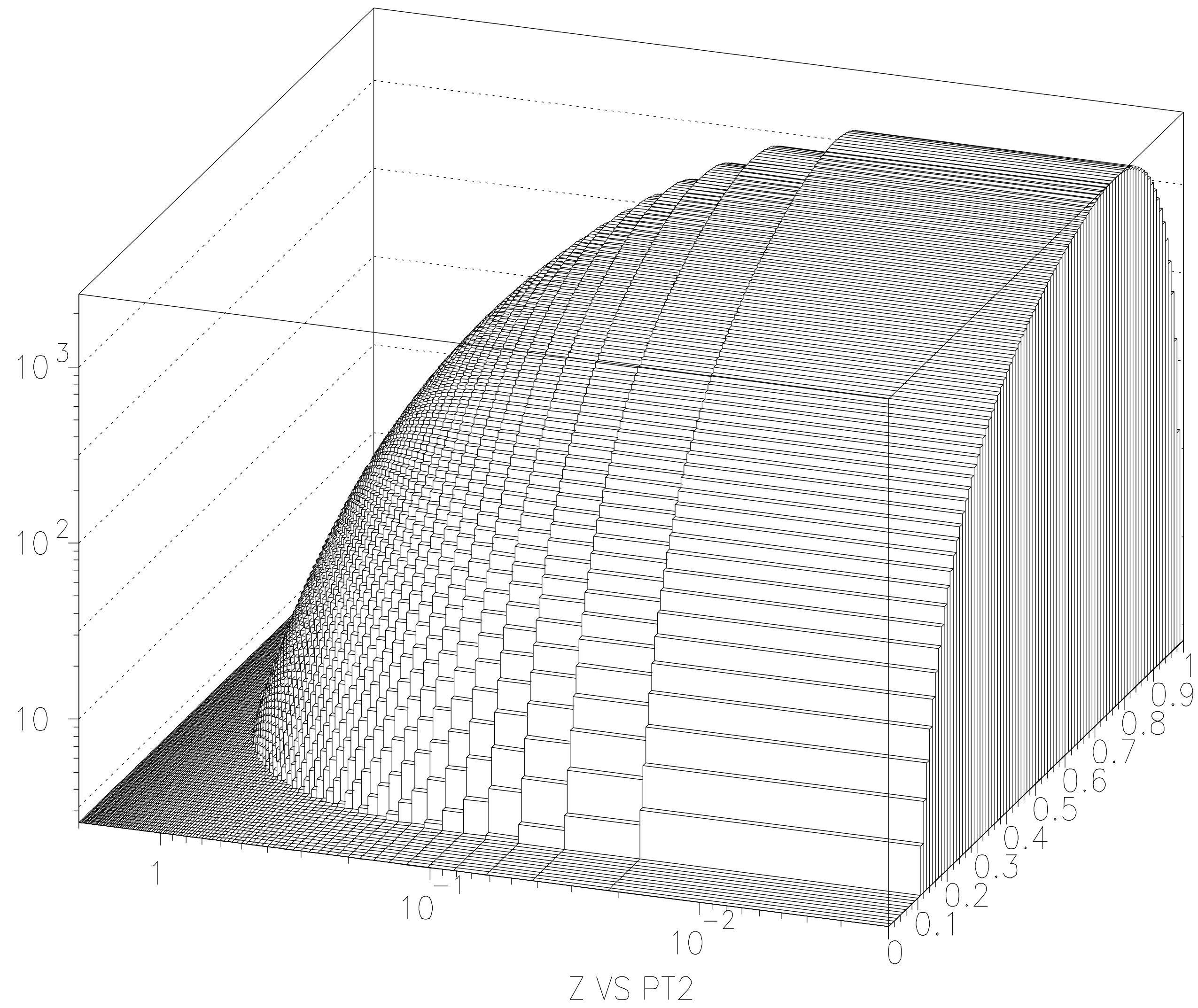

FIG. 4. The pion exchange cross section $d\sigma(ep \to e'nX)/dx\, dQ^2\, dz\, dp_T^2$ in units of nb/GeV^4 evaluated at $x = 0.001$ and $Q^2 = 10$ GeV^2.

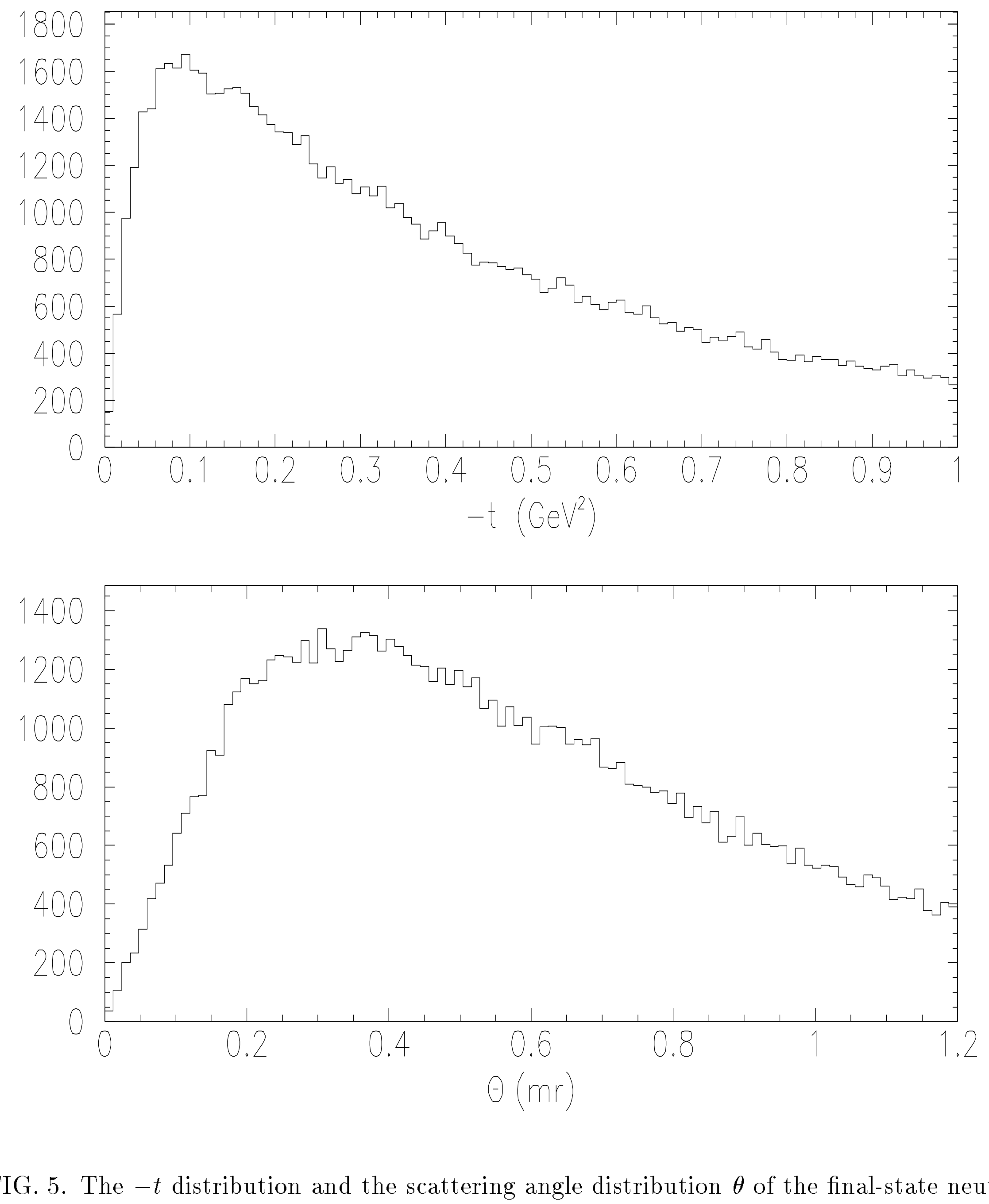

FIG. 5. The $-t$ distribution and the scattering angle distribution θ of the final-state neutrons. The figures were generated using Equation 5 evaluated at $x = 0.001$ and $Q^2 = 10$ GeV^2.

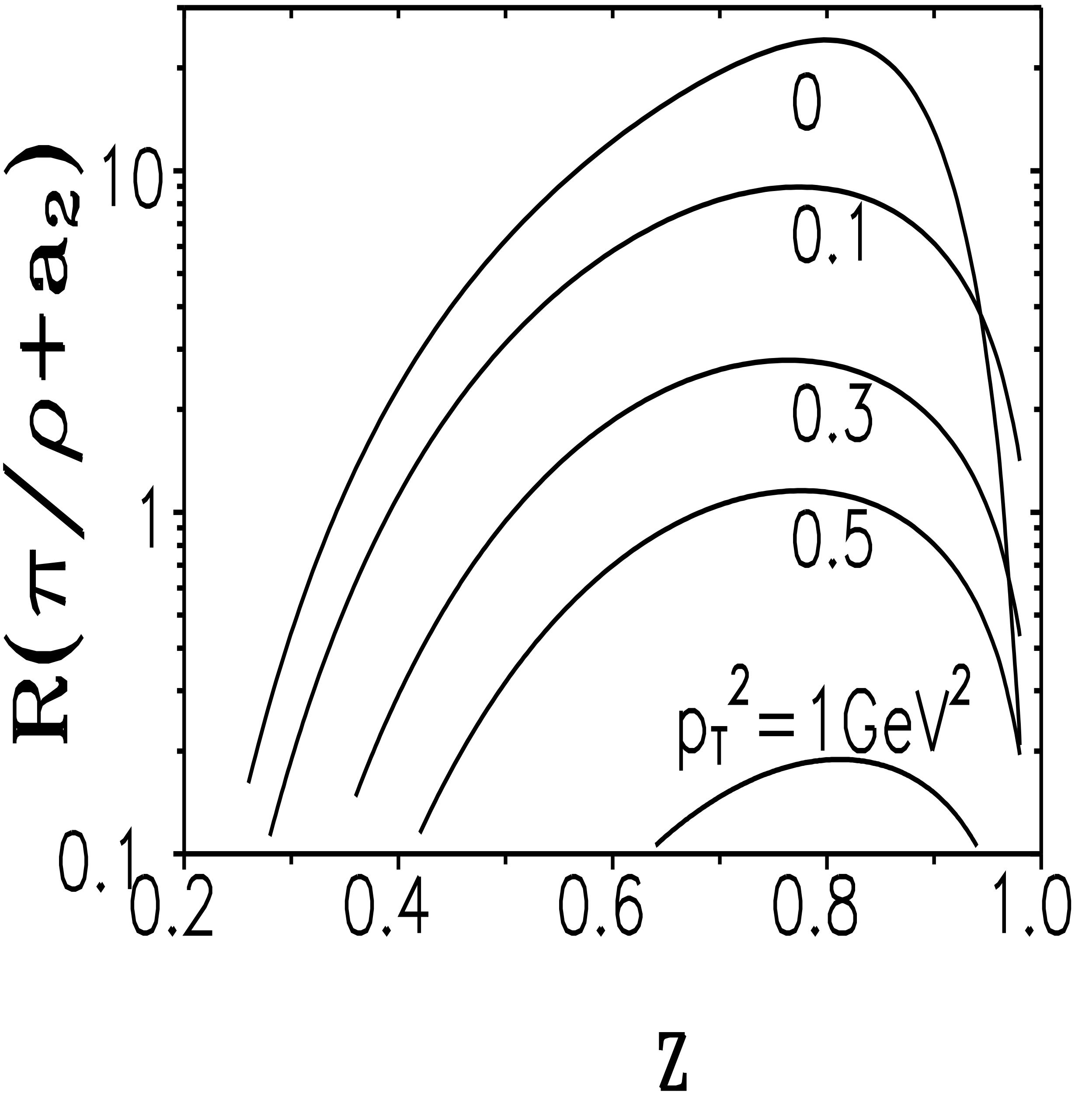

FIG. 6. Ratio of pion-exchange contribution to $dF_2^{p\to n}(x,Q^2)/dzdp_T^2$ and the background, provided by ρ and a_2 exchanges, as functions of z. The ratio is shown for different values of the transverse momentum p_T^2.

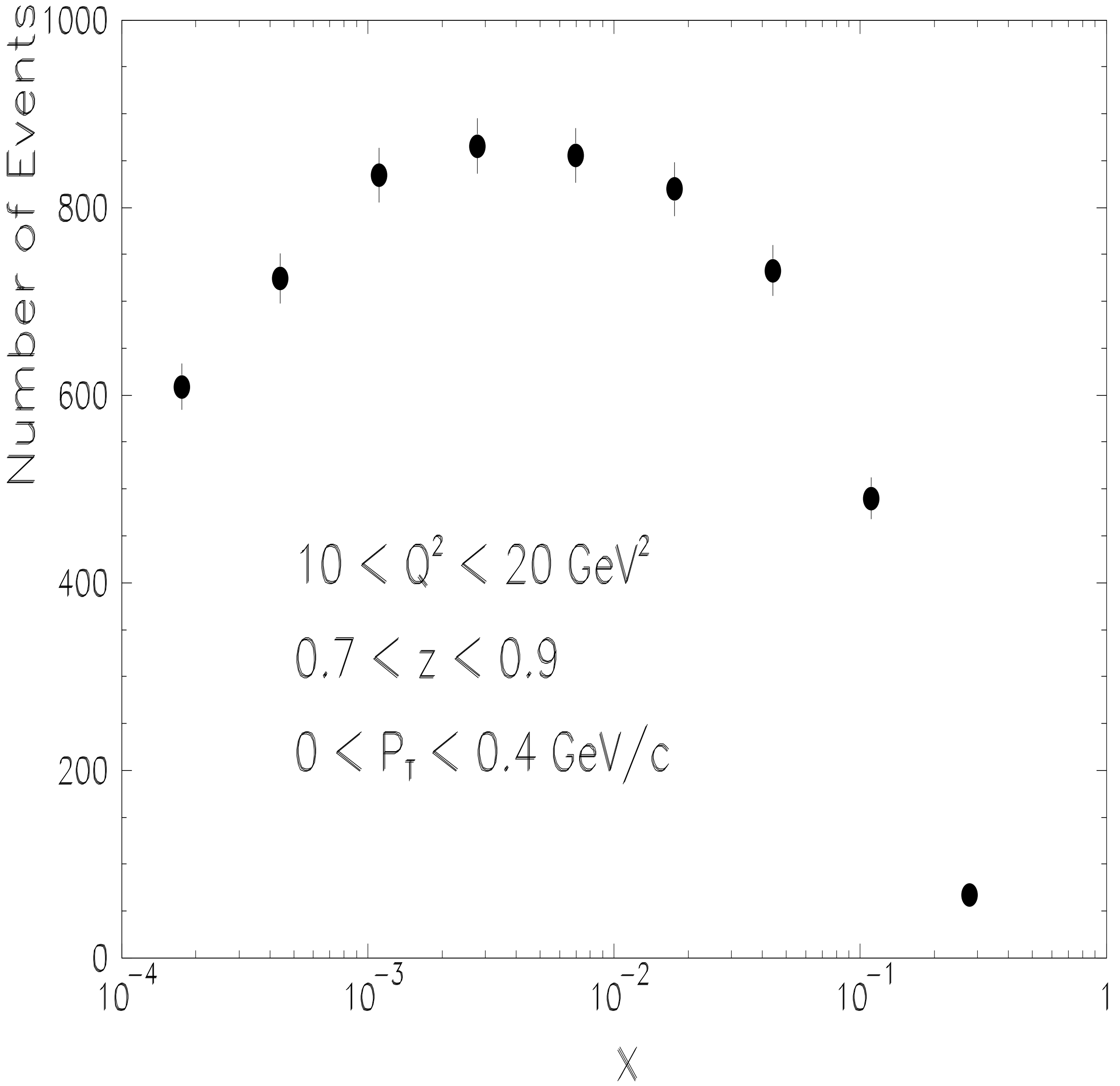

FIG. 7. The expected number of reconstructed events within the limited kinematic range $0.7 < z < 0.9$, $10 < Q^2 < 20$ GeV^2, and $0 < p_T^2 < 0.16$ (GeV/c)^2. An integrated luminosity of 10 pb^{-1} and an acceptance of 50% have been assumed.

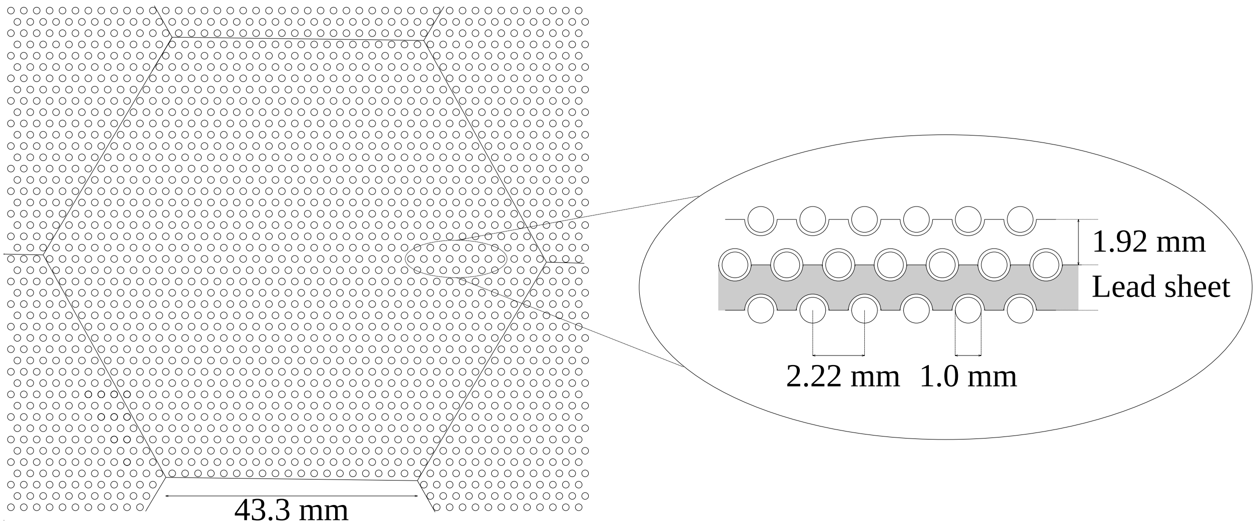

FIG. 8. Layout of the SPACAL Pb/scintillating fiber matrix. The hexagonal tower structure is obtained by coupling 1141 fibers to a common PM.

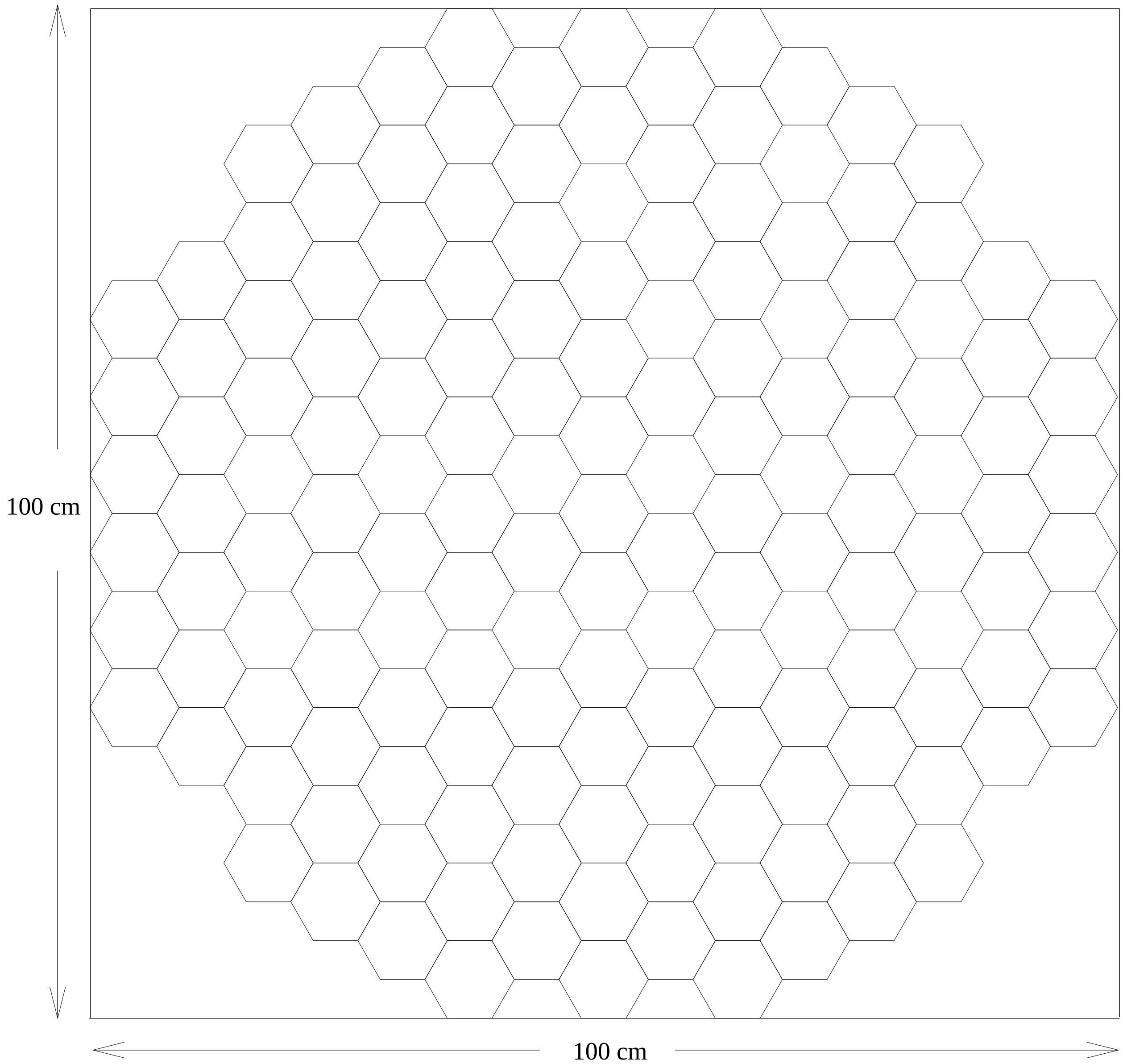

FIG. 9. Front view of the SPACAL. Shown is the lateral segmentation of the calorimeter in 155 hexagonal towers.

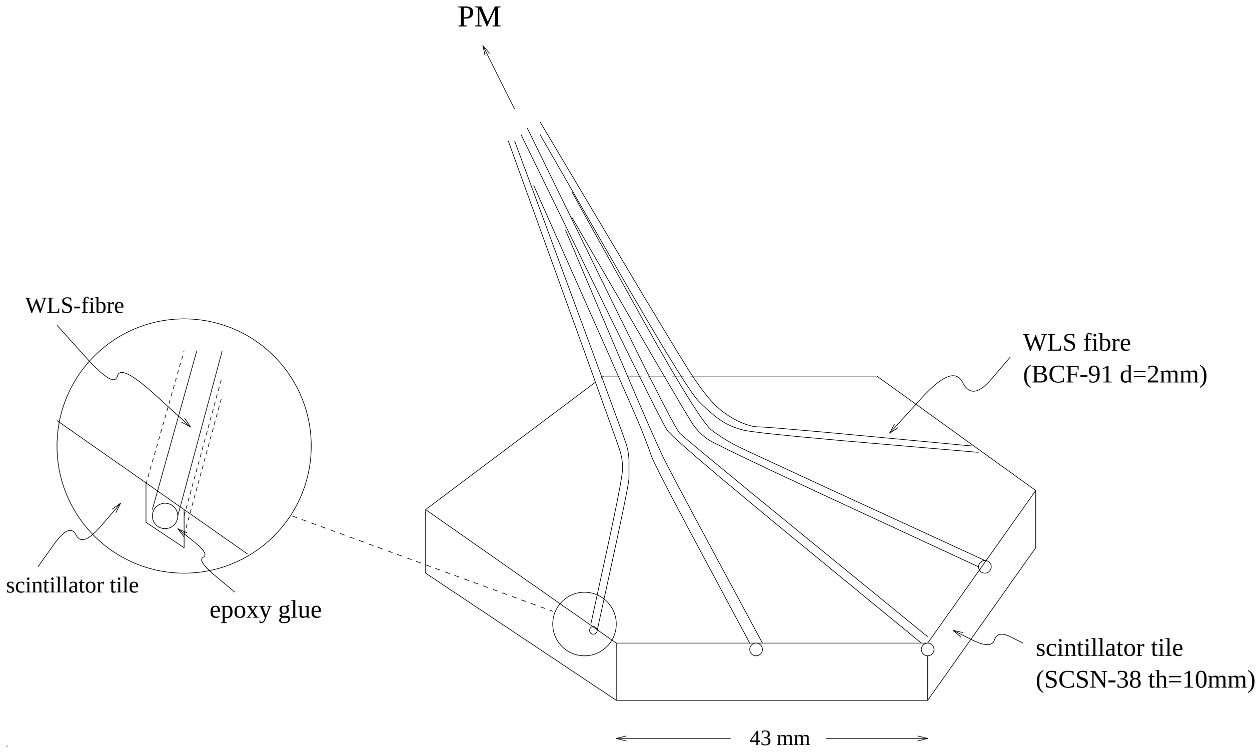

FIG. 10. Layout of a scintillator tile. Light produced by a particle traversing the scintillator is absorbed by 5 wave length shifting fibers and guided to the PM.

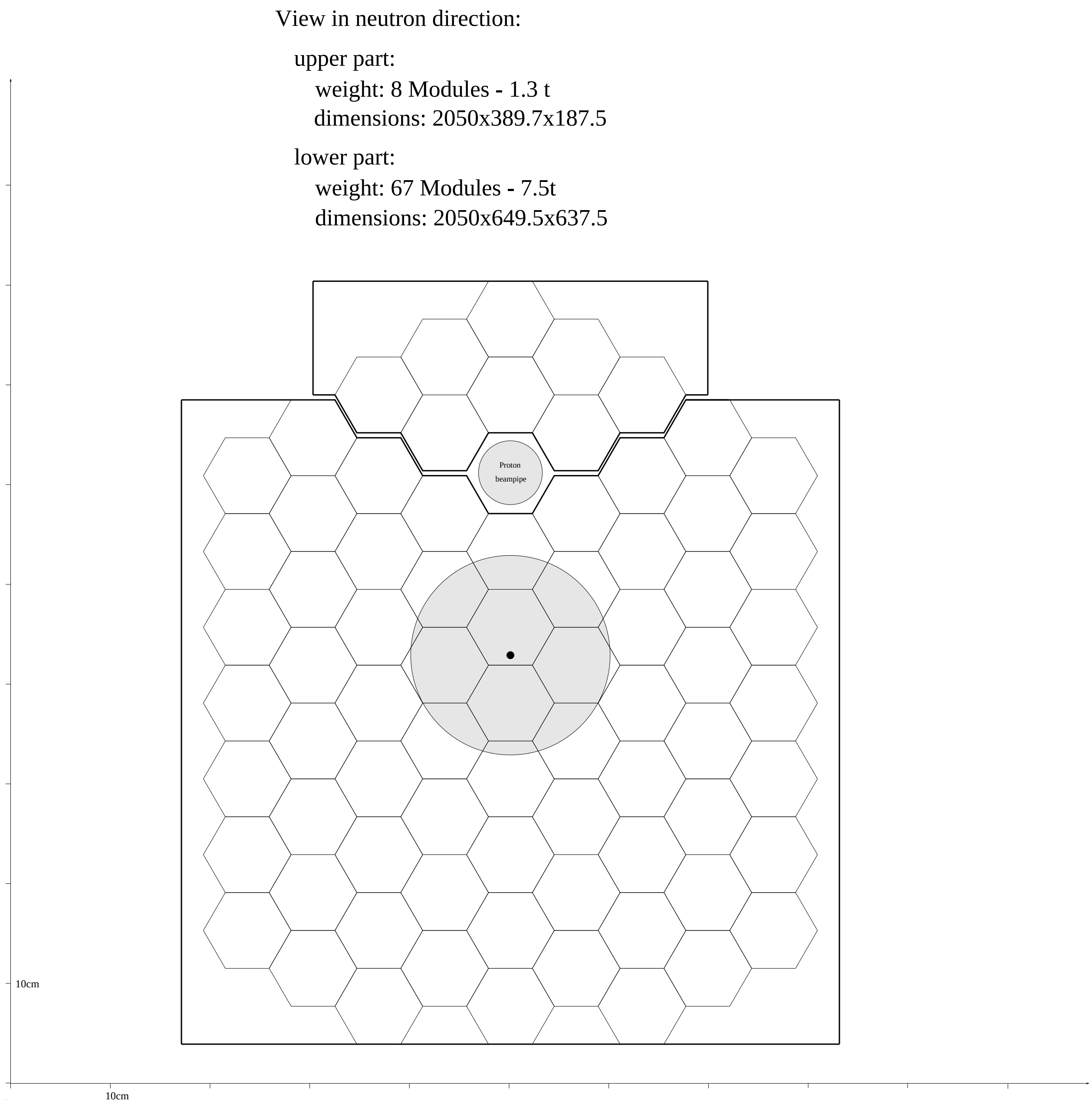

FIG. 11. Configuration of the forward neutron calorimeter.

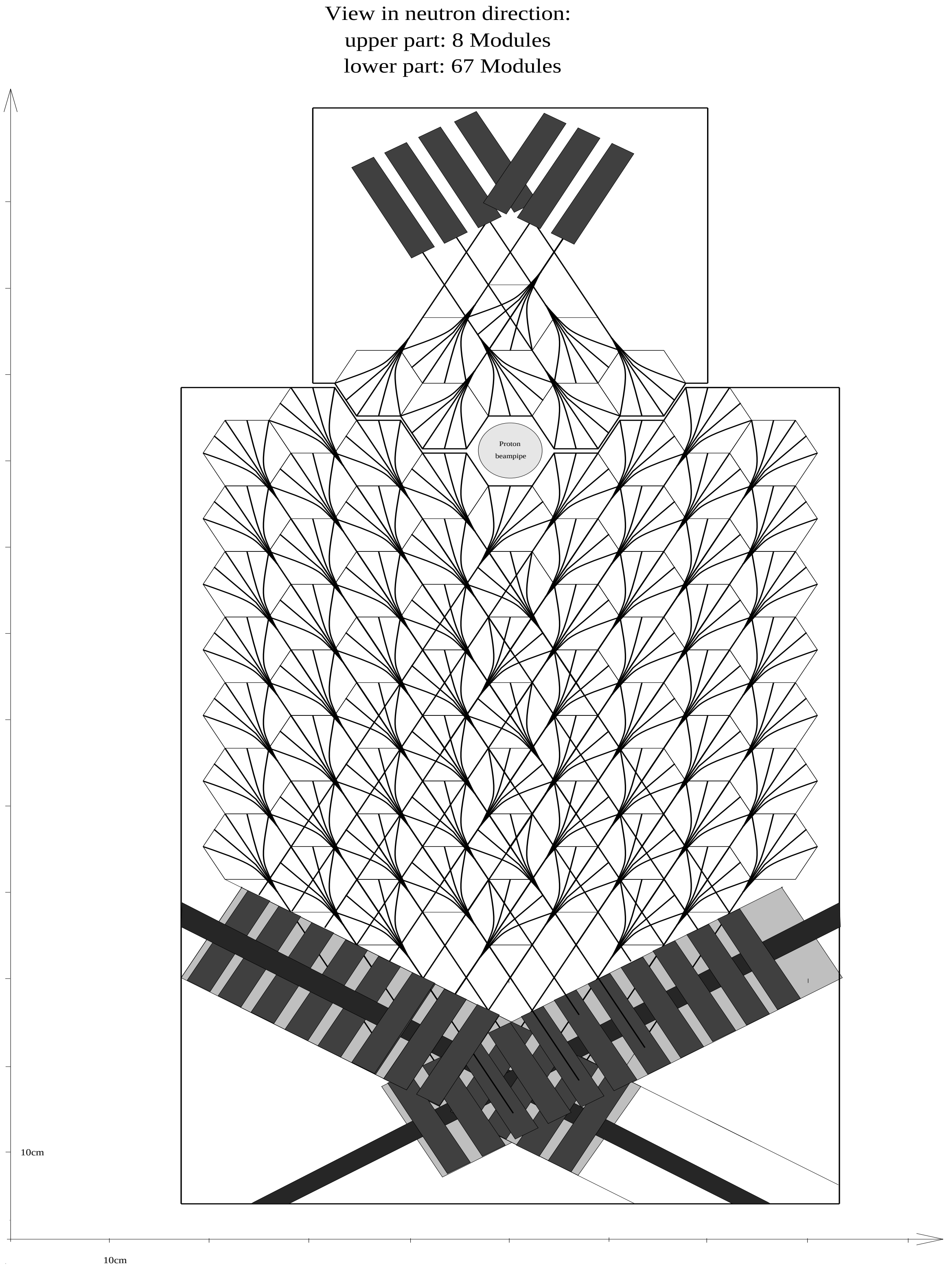

FIG. 12. Hodoscope configuration for the neutron calorimeter.